iScience

Article

Virtual patients inspired by multiomics predict the efficacy of an anti-IFNα mAb in cutaneous lupus

Graphical abstract

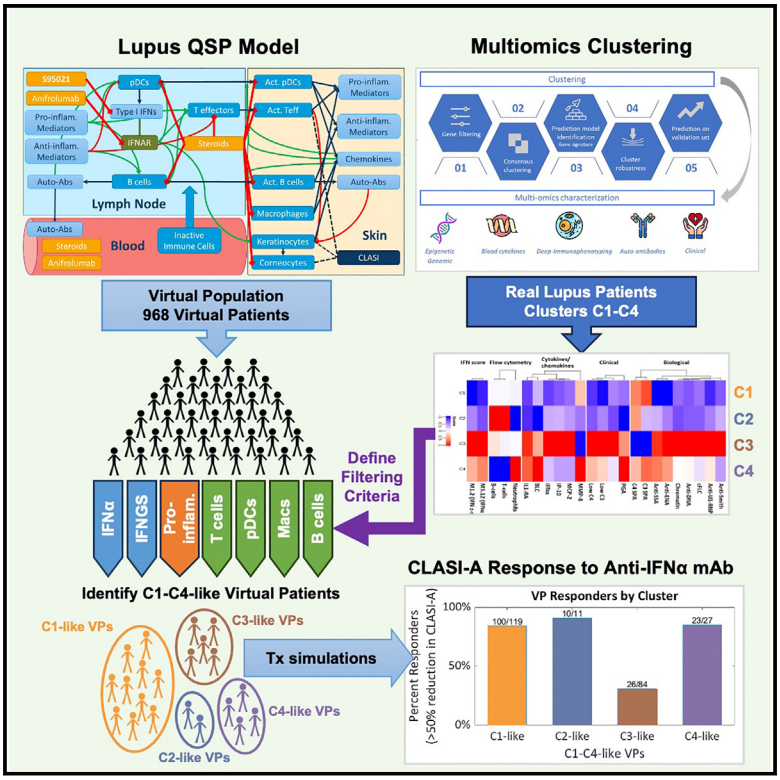

Highlights

- QSP modeling of lupus can be used to predict the efficacy of drug candidates
- A cohort of virtual lupus patients was created from profiling data of actual patients
- Virtual patient simulations predicted distinct anti IFN treatment responses
- Machine learning found biomarkers to differentiate responders from non-responders

Authors

Vincent Hurez, Glenn Gauderat, Perrine Soret, ..., Sylvain Fouliard, Philippe Moingeon, the PRECISESADS Clinical Consortium

Correspondence

vincent.hurez@regeneron.com (V.H.), philippe.moingeon@universite-paris-saclay.fr (P.M.)

In brief

In silico biology; Biological constraints; Omics; Machine learning; Computer simulation

Hurez et al., 2025, iScience *28*, 111754
February 21, 2025
https://doi.org/10.1016/j.isci.2025.111754

CellPress

iScience

CellPress
OPEN ACCESS

Article

Virtual patients inspired by multiomics predict the efficacy of an anti-IFNα mAb in cutaneous lupus

Vincent Hurez,[1,5,*] Glenn Gauderat,[2] Perrine Soret,[2] Renee Myers,[1] Krishnakant Dasika,[1] Robert Sheehan,[1] Christina Friedrich,[1] Mike Reed,[1] Laurence Laigle,[2] Marta Alarcón Riquelme,[3] Audrey Aussy,[2] Loubna Chadli,[2] Sandra Hubert,[2] Emiko Desvaux,[2] Sylvain Fouliard,[2] Philippe Moingeon,[2,4,6,*] and the PRECISESADS Clinical Consortium

[1]Rosa and Co. LLC, San Carlos, CA, USA
[2]Servier, Research and Development, Saclay, France
[3]GENYO Center for Genomics and Oncological Research, Granada, Spain
[4]Present address University Paris Saclay, Orsay, France
[5]Present address: Regeneron Pharmaceuticals, Tarrytown, NY, USA
[6]Lead contact
*Correspondence: vincent.hurez@regeneron.com (V.H.), philippe.moingeon@universite-paris-saclay.fr (P.M.)
https://doi.org/10.1016/j.isci.2025.111754

SUMMARY

Lupus erythematosus is a heterogeneous autoimmune disease that requires treatments tailored to specific patient subsets. To evaluate *in silico* the efficacy of the anti-IFNα S95021 monoclonal antibody, we created a quantitative systems pharmacology model of cutaneous lupus and a virtual patient population, with attributes matching the diversity of actual patients. To this aim, we performed a multiomics profiling analysis of 337 lupus patients from the PRECISESADS cohort, thereby identifying four patient clusters with distinct immune dysregulation patterns, including various levels of type I interferon (IFN) pathway upregulation. Simulation of S95021 treatment in the virtual patient cohort ($n = 241$) predicted distinct clinical responses in patient clusters, with machine learning analysis further revealing biomarkers that distinguish predicted responders from non-responders. Combining multiomics profiling of actual patients with mechanistic mathematical modeling supports precision medicine by predicting drug responses based upon patient characteristics in a complex heterogeneous disease.

INTRODUCTION

Systemic lupus erythematosus (SLE) is a heterogeneous multi-organ autoimmune disease affecting predominantly the joints, skin, and kidney.[1,2] Several immunosuppressive therapies have long been used to alleviate symptoms, demonstrating variable efficacy across patients while inducing significant side effects.[3–5] Better understanding of pathophysiological mechanisms associated with lupus, involving most particularly pathogenic autoantibodies and elevated levels of type I interferons (IFN), led to the development of targeted biotherapies using monoclonal antibodies such as the anti-B-cell activating factor (BAFF) belimumab and the anti-type I IFN receptor (IFNAR) anifrolumab, recently registered as treatments for severe to moderate lupus.[5–10] Positive results in several clinical trials with anifrolumab, together with evidence that IFN levels may correlate with disease activity in some patients, confirmed that type I IFNs are a valid therapeutic target in lupus.[11–14] Surprisingly, only 50% of patients benefited from anifrolumab in the phase III trials, despite the fact that about 82% of them exhibit a constitutive activation of the type I IFN pathway.[8–10]

These observations reflect the heterogeneous nature of this disease, with a dysregulation of multiple pro-inflammatory molecular pathways associated with innate or adaptative immunity depending upon the patient.[15–21] Such complexity in the pathophysiology has also been reported in several other autoimmune diseases, such as Sjogren disease, rheumatoid arthritis, and systemic sclerosis.[22–25] In this context, an emerging consensus is to implement a precision medicine approach to develop next-generation treatments for autoimmune rheumatic diseases, including lupus.[23,26–28] By offering treatments better tailored to homogeneous subgroups of patients based upon shared underlying pathogenic disease mechanisms, precision medicine is now considered the "holy grail" in clinical care of systemic autoimmune rheumatic diseases.[28] The latter approach requires sophisticated stratification approaches based on multiomics profiling to document patient heterogeneity, validate therapeutic targets, and identify predictive molecular signatures of drug response.[29–34] Furthermore, given the complexity of autoimmune diseases such as SLE, most appropriate treatments may ideally rely upon combination therapies, as opposed to standalone targeted drugs.[25]

Whereas investigating those questions solely based on real-world preclinical and clinical research activities remains extremely challenging, computer-aided modeling powered by artificial intelligence (AI) is now becoming available to select initial working hypotheses, which can subsequently be confirmed in empirical studies, with a higher probability of success.[24,25] Computational precision medicine refers to the emerging use of multiple predictive models to relate patient specificities with drug properties, in order to inform drug development and positioning.[35] Among those, quantitative systems pharmacology (QSP) models are mechanistic representations of disease pathophysiology linking

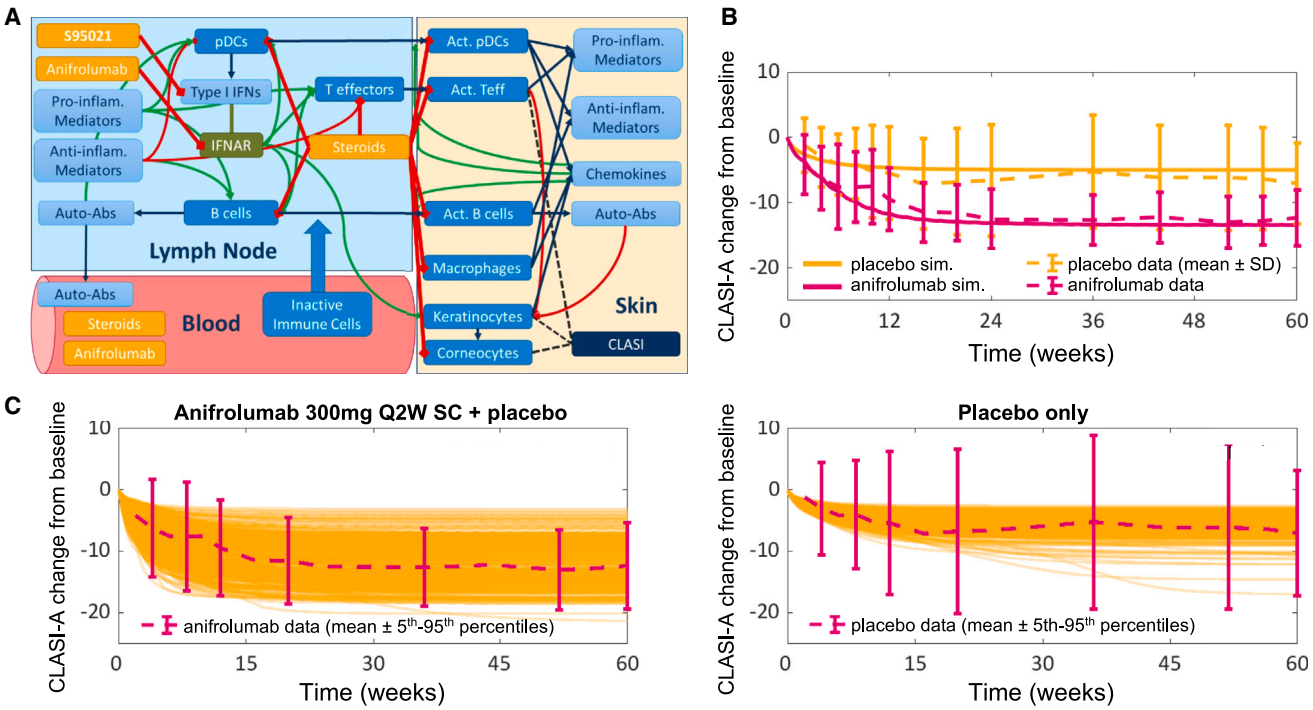

Figure 1. QSP model simulations match reported clinical responses to anifrolumab

(A) Schematic of the components of the lupus QSP model and their interactions.

(B) Simulations of changes in CLASI-A with placebo only (orange line) or 300 mg anifrolumab + placebo administered every two weeks via the subcutaneous route (pink line) in the reference VP match the average clinical response in the anifrolumab-treated or placebo groups (dashed lines, mean ± SD from[48]).

(C) CLASI-A changes with 300 mg anifrolumab + placebo administered every two weeks via the subcutaneous route (left panel) or with placebo only (right panel) simulated for 968 individual VPs are consistent with the clinical response in anifrolumab-treated patient or the placebo group. The predicted responses to anifrolumab in the 968 VPs (left panel: orange lines) span the range of response measured in a published clinical trial (dashed lines, mean ± 5th–95th percentiles from the study by Bruce et al.[48]).

biological processes occurring in the blood or target tissues with clinical symptoms.[36–41] Such QSP models have successfully been used to predict the efficacy of drug candidates in various autoimmune and chronic inflammatory diseases.[42–47]

Herein, we report on a multipronged modeling strategy to predict the efficacy in cutaneous lupus erythematosus (CLE) of the pan neutralizing anti-IFNα monoclonal antibody (mAb) S95021,[11] in comparison with anifrolumab, across patient heterogeneity. To this aim, we built a QSP model of CLE representing biological processes occurring in skin and draining lymph nodes related to cutaneous symptoms. In parallel, we documented the heterogeneity of lupus patients by clustering patients based on multiomics molecular profiling data in the blood. We took advantage of this combined approach to create a cohort of virtual patients representing the heterogeneity observed across four clusters identified among lupus patients, to predict *in silico* the efficacy of the S95021 mAb across inter-individual variability.

RESULTS

Development of a cutaneous lupus QSP model and virtual patient population

As a first step, a mechanistic QSP model representing the major cellular dynamics and regulations involved in cutaneous lupus manifestations was developed (Figure 1A) and qualified according to our previously published methodology.[36] Model parameters were identified from literature and calibrated to represent an average moderate lupus patient with cutaneous symptoms, subsequently termed "reference virtual patient" (reference VP)(see STAR Methods). Target values for model species, such as the numbers of infiltrating immune cells (dendritic cells, macrophages, T and B lymphocytes) in lymph nodes and skin, were averaged from studies in lupus patients when available (Tables S1–S5). Alternatively, data from lymph nodes or skin of healthy individuals were used, with further estimation of fold changes occurring in lupus patients. Immune cells and keratinocyte dynamics were calibrated to be consistent with biological and modeling constraints (Tables S1A, S1B, S1C, and S1D). For example, cell proliferation and recruitment rates were adjusted to balance out cell clearance rates in the skin and lymph node compartments to maintain appropriate stable cell numbers at steady state.

Pharmacokinetics and pharmacodynamics properties of the anti-IFNα S95021 and the approved anti-IFNAR anifrolumab monoclonal antibodies were implemented in the QSP model. A generic immunosuppressive effect ("placebo") based on steroid *in vitro* data (Table S6) was simulated at constant levels to reproduce the overall clinical response observed in patients treated

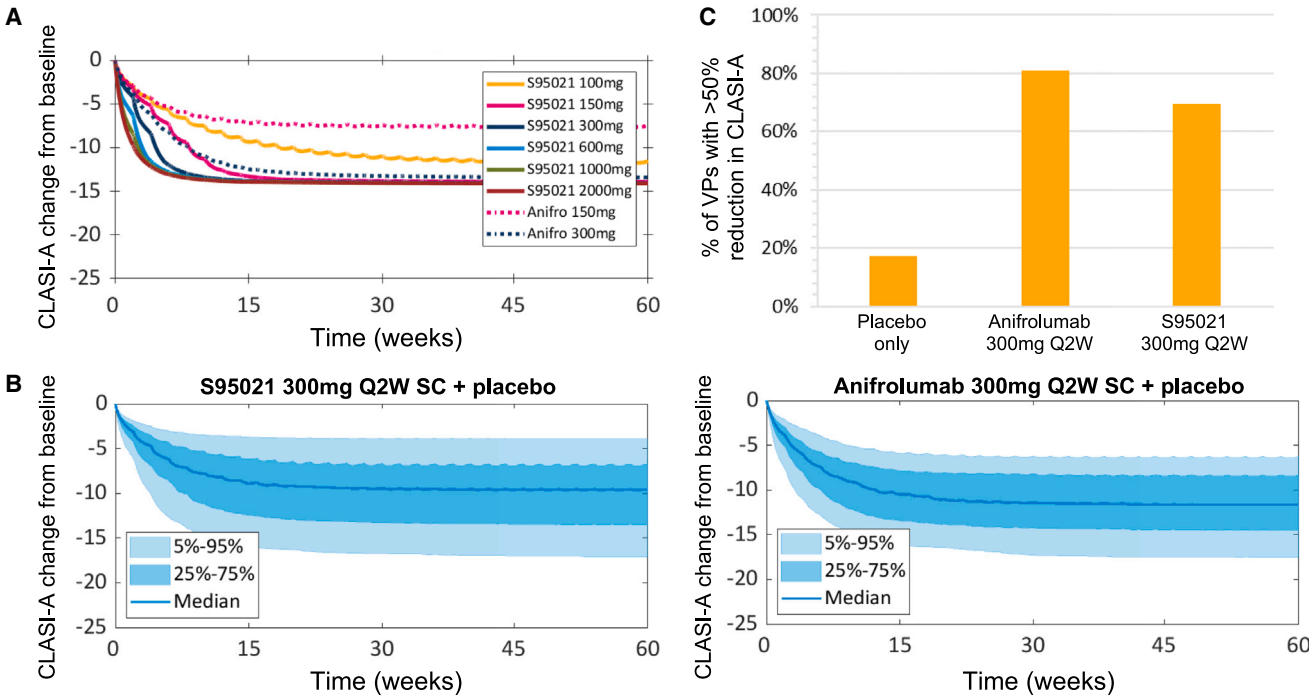

Figure 2. Comparative assessment of S95021 and anifrolumab in the QSP lupus model

(A) Significant decrease in CLASI-A simulations in the reference VP treated with 100–2000 mg S95021 + placebo (plain lines) or 150–300 mg anifrolumab + placebo (dashed lines) with Q2W SC dosing.

(B) Change in CLASI-A simulations with S95021 300mg Q2W SC + placebo (left panel) or 300 mg anifrolumab Q2W SC + placebo (right panel) in the Vpop. The median change in CLASI (blue line), quartiles (25%–75%) and 5th–95th percentiles for the Vpop are represented.

(C) Percentages of VPs in the total Vpop with predicted decrease from baseline in CLASI-A greater than 50% at 60 weeks with placebo only, 300 mg anifrolumab + placebo, or 300 mg S95021 + placebo treatments.

with various background therapies (such as steroids, immunosuppressive drugs, and hydroxychloroquine) in the placebo group from published clinical trials. The cutaneous lupus erythematosus disease area and severity index (CLASI)[49] was calculated as the primary clinical endpoint in the QSP model by correlating model species (cell numbers, mediator levels) with individual CLASI score components (see STAR Methods). The clinical responses to anifrolumab (administered at 300 mg every two weeks via the subcutaneous route, subsequently abbreviated Q2W SC) + placebo or to placebo only treatment were simulated in the reference VP (Figure 1B, Table S6). Predicted responses were calibrated to match the average CLASI response measured in the anifrolumab and the placebo group, respectively, in a published phase 2 clinical trial in moderate to severe lupus patients (CLASI score > 10)[6,48,49] (Figure 1B).

Following confirmation of the calibration of the QSP model by congruence with published clinical data, we created virtual patients. Starting with the average parameter values defining the reference VP, a large cohort of VPs was produced by randomly varying critical parameters in the model, using a range of values estimated from published pre-clinical and clinical studies (Tables S1C). Among tens of thousands of randomly created VPs, a virtual population (Vpop) of 968 VPs was selected, as they met defined biological constraints such as cell numbers in lymph nodes and skin, as well as ranges of baseline CLASI scores, consistent with real lupus patient features described in the literature or enrolled in recent clinical trials (Tables S1A and S1D). Specifically, the Vpop was fitted to a normal distribution for (1) CLASI baseline distribution and (2) change in CLASI score at 60 weeks in the anifrolumab and placebo-treated groups from the phase 2 anifrolumab study[6] (STAR Methods). The baseline CLASI distribution in the Vpop was consistent with the baseline CLASI score of 15.5 ± 5.2 reported in the phase 2 anifrolumab trial (Table S7).[6]

Using this Vpop, we then ran simulations of treatments with either 300 mg anifrolumab Q2W SC + placebo or background placebo only, in comparison with the CLASI response over time observed in the published phase 2 anifrolumab trial (Figure 1C). The predicted CLASI response of the 968 individual VPs to anifrolumab treatment reflected the range of responses observed in the anifrolumab-treated group (Figure 1C, left panel), confirming that the Vpop is representative of the diversity of response observed in real lupus patients enrolled in the trial. Simulations of the response to placebo only in the Vpop also agreed with published clinical data, albeit exhibiting less variability in CLASI responses than observed in the clinical trial placebo group (Figure 1C, right panel). A potential explanation is that the placebo response observed in real lupus patients stems from different background therapies in terms of drugs and dosing regimens and/or drug-independent effects, which can

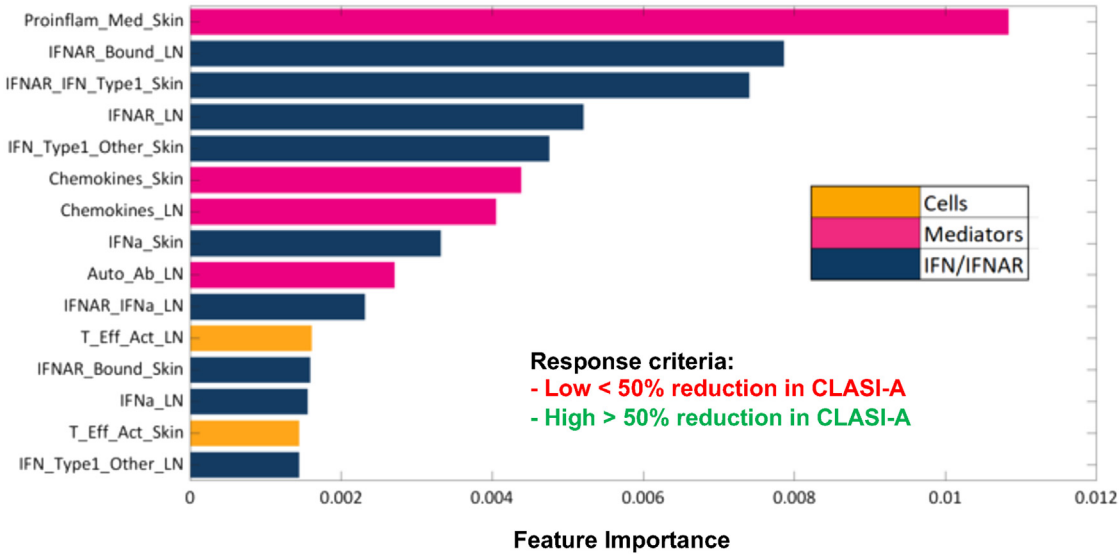

Figure 3. Tree ensemble analysis ranks pro-inflammatory mediators and IFN signaling as critical features for clinical response to S95021

Tree ensemble analysis showing the top 15 model features ranked by order of importance distinguishing VPs with low vs. high CLASI response to S95021.

only be partially reflected by simulating the response to a generic placebo immunosuppressive effect in the Vpop. This variability in placebo responses in real-world clinical studies consequent to a lack of standardization of background therapies—both in terms of drugs and dosing being used—is well identified as a significant hurdle in the evaluation of investigational drugs against autoimmune diseases.[50,51]

Predictive simulations for S95021 CLASI responses

Following validation of the QSP lupus model using the anifrolumab published data, we evaluated the efficacy of S95021, a novel pan-neutralizing anti-IFNα mAb,[11] as a potential treatment for cutaneous lupus. The model was used to compare the reduction in the CLASI score elicited with either S95021 (at doses ranging from 100 mg to 2,000 mg) or anifrolumab (150 or 300 mg), when administered on top of placebo every two weeks via the subcutaneous route (Q2W SC) (Figure 2A). Simulations in the reference VP showed that CLASI-A responses were predicted to be quite comparable, both in terms of magnitude and time course, when using 150 mg S95021 or 300 mg anifrolumab Q2W SC (Figure 2A). In the reference VP, the maximum CLASI-A response for both anifrolumab and S95021 was reached with the 300 mg Q2W SC dosing, although this maximum was reached faster with 300 mg S95021 (Figure 2A).

The efficacy of S95021 or anifrolumab, plus placebo, was then evaluated in the Vpop using the approved anifrolumab clinical dosing (300 mg Q2W SC) and 60 week of treatment duration for both drugs (Figure 2B). In the Vpop, the CLASI response to 300 mg S95021 was predicted to be lower than with 300 mg anifrolumab: average decrease in CLASI-A of -9.7 ± 4 with S95021 versus -10.5 ± 3 with anifrolumab (p value < 0.001). As primary clinical endpoints in lupus trials are often reported as percentage of patients achieving a significant improvement in the CLASI score,[6] we calculated the percentages of VPs with greater than 50% reduction in CLASI-A from baseline: respectively 17%, 81%, and 70% of the 968 VPs were predicted to exhibit such a response with placebo, anifrolumab, or S95021 (Figure 2C). The Vpop simulations suggest that some lupus patients could benefit from dosing regimens greater than 300 mg SC for S95021 to achieve clinical response equivalent to anifrolumab.

To further analyze the drivers of S95021 clinical response in the whole Vpop, we implemented a decision tree analysis to investigate attributes associated with predicted anti-IFN therapy efficacy. Using MATLAB machine learning tools, we identified model species that were differentiating VPs with predicted low versus high response to S95021 in the Vpop, based on the CLASI response criteria defined above (> 50% reduction in CLASI-A). Tree ensemble analysis ranked skin pro-inflammatory mediators, IFNs/IFNAR signaling, and skin and lymph node (LN) chemokines as highly predictive biomarkers of S95021 response (Figure 3). Cellular infiltrates by effector T cells in skin and lymph nodes were also ranked in the top 15 features predicting high versus low CLASI responses to S95021.

Surprisingly, single decision tree analysis (Figure S1) predicted that very high levels of IFNα or bound IFNAR:IFNα complex were associated with low CLASI response to 300 mg S95021, likely because IFN inhibition under these conditions may not be sufficient in patients with very high levels of type I IFN signaling. Thus, patients with strong type I IFN involvement may potentially benefit from higher dosing of S95021 to fully control disease activity.

Assessment of real lupus patient heterogeneity by multiomics profiling of the PRECISESADS cohort

To further optimize the design and selection of VPs to model drug efficacy, we assessed patient heterogeneity using a large multiomics dataset from the cross-sectional PRECISESADS cohort,[30,31] obtained from the blood of 337 lupus patients in comparison with 330 healthy volunteers. Applying our strategy previously used to categorize Sjogren patients,[23] we first relied

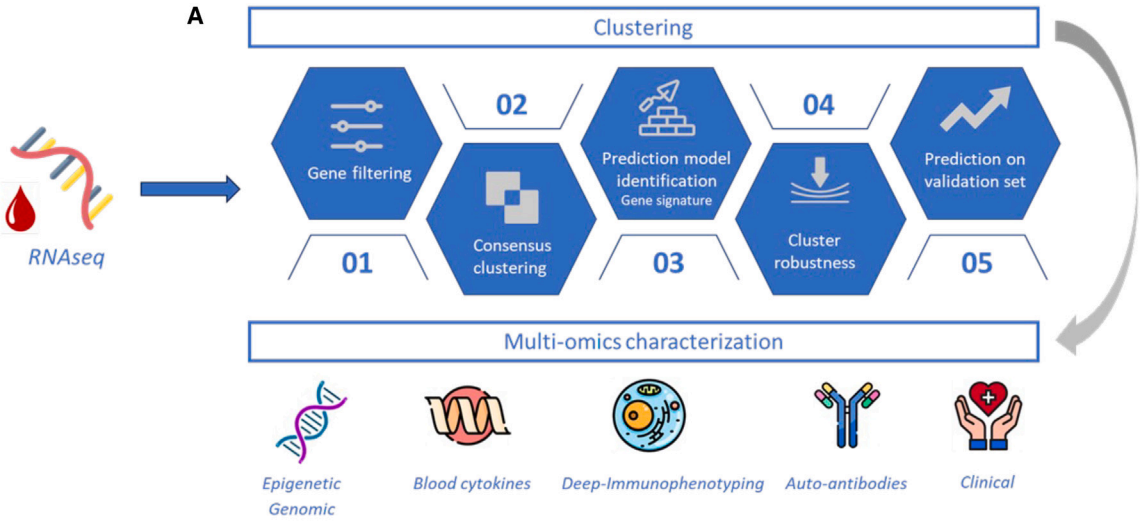

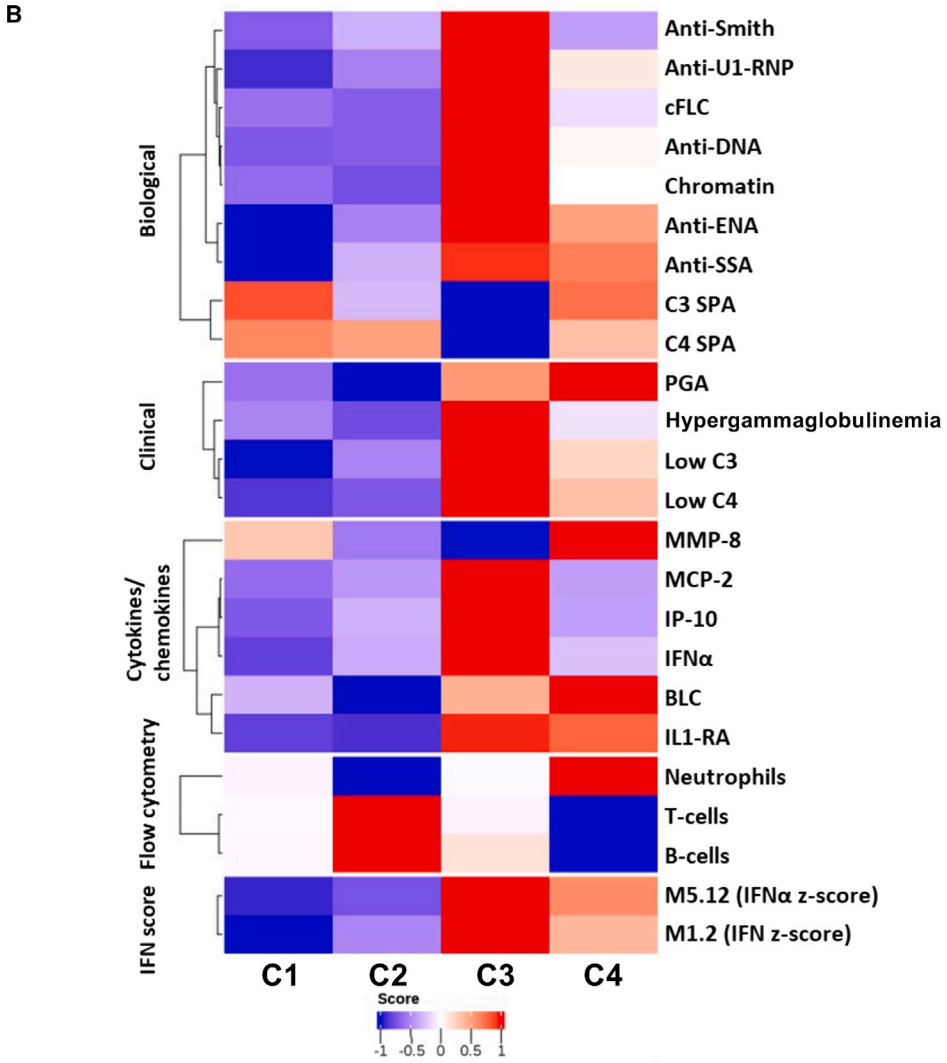

(legend on next page)

upon transcriptomics data from the blood and used an in-depth machine learning analysis combined with unsupervised and supervised clustering approaches to stratify lupus patients into homogeneous clusters. Patient characteristics within each cluster were further documented based on genomic, epigenetic, deep immunophenotyping analyses, quantification of cytokines and chemokines, as well as clinical phenotyping (Figure 4A, See STAR Methods).

Molecular profiling and clustering studies identified four subgroups of SLE patients, with distinct phenotypic features of clusters summarized in a heatmap (Figure 4B). Cluster 1 (C1) contained 95 patients (28.1%), cluster 2 (C2) 103 patients (30.5%), cluster 3 (C3) 66 patients (19.5%), and cluster 4 (C4) 73 patients (21.7%). Schematically, the four clusters of lupus patients can be labeled as mild disease (C1), lymphoid (C2), interferon high (C3), and inflammatory (C4). All descriptive statistics regarding clinical features and biological parameters as well as main characteristics for each of the clusters are reported in detail in Tables S8 and S9.

When assessing covariates driving the clustering, we observed significant differences between clusters in concentrations of extractable nuclear antigen (ENA), presence of serum anti-SSA52/anti-SSA60 autoantibodies, and levels of pro-inflammatory cytokines (e.g., MCP-2, IP10, IFNγ, and IL1-RA), all higher in C3 compared to other clusters (Table S9). Differences in circulating leukocyte subsets were also found between clusters. An increase in neutrophils and a decrease in T and B lymphocyte frequencies were observed in C4, with an opposite distribution of those immune cell subsets found in C2. To document IFN gene signatures (IFNGS) in the various patient clusters, we took advantage of two strongly upregulated IFN-annotated gene modules (termed M1.2 and M5.12) identified by Chiche et al. from peripheral blood transcriptomic data, with for each module a distinct activation threshold.[52] Genes within the M1.2 module are induced by IFNα or IFNβ, corresponding to a type I IFN signature. Genes from the M5.12 module are poorly induced by IFNα and IFNβ alone, but are up-regulated by IFNγ, thus rather reflecting a type II IFN signature. The different *Z* scores for those genes were calculated accordingly to characterize the IFN signature observed in the various PRECISESADS clusters. Whereas the IFN *Z* scores were elevated in all clusters, a stronger signal was observed in C3 and C4, relative to C1 and C2. No differences were detected between type 1 and type II IFN *Z* scores. Distribution in cell numbers, IFN levels, IFNGS, and cytokines for the four SLE clusters are reported in Figures S2–S4.

Matching virtual patients to PRECISESADS actual patient clusters

In order to assess which of the four lupus patient clusters previously defined would benefit the most from an anti-IFN therapy, we proceeded to determine which VPs could be matched to real patients from the C1 to C4 clusters. To this aim, we identified the model species represented in the QSP model that could be mapped to cellular or biological biomarkers measured in PRECISESADS lupus patients. From this, we selected seven baseline species to use as filter criteria to identify VPs matching the C1 to C4 clusters (Figure 5A). The range of values for each species in each cluster was defined based on the mean and distribution of the associated features measured in patients from the four PRECISESADS clusters, such as IFNα and IFNGS, immune cells as well as cytokines and mediators in the blood, or pro-inflammatory and anti-inflammatory mediators in the skin (Figures S2–S5). Filter criteria were more stringent for attributes that had the highest impact on CLASI score, as determined by ensemble decision tree analysis (see STAR Methods). Using these filtering criteria on the whole VP cohort, we identified a total of 241 VPs that matched the phenotypes of the four PRECISESADS clusters defined previously (Figure 5B).

Evaluation of the S95021 clinical response in VPs matching PRECISESADS clusters

We confirmed that the VPs selected using the filtering criteria reported in Figure 5A were consistent with the distribution for the corresponding biomarkers in the C1–C4 clusters of actual lupus patients. For example, the levels of skin IFNα and IFNAR/IFNα complexes (IFNAR-bound_in the skin) were low in the VPs corresponding to clusters C1 and C2, medium in C3-like VPs and very high in C4-like VPs, consistent with the distribution observed for plasma IFNα and IFNGS in actual patients (Figures 6A and 6B). The relative levels of pro-inflammatory and anti-inflammatory mediators in the C1–C4-like VPs were also generally consistent with the distribution observed in real patients for plasma tumor necrosis factor alpha (TNF-α) and transforming growth factor β (TGF-β), respectively, with C1-like and C3-like VPs showing slightly higher levels of pro- and anti-inflammatory mediators compared to C2 and C4-like VPs (Figure S5). With the hypothesis that the lymphopenia and leukopenia observed in lupus patients results from increased recruitment of immune cells to the site of inflammation, we defined thresholds for skin cell infiltration to filter VPs based on the relative decrease in corresponding cell types in the blood of PRECISESADS patients (Figures 5B and S6).

We then simulated the CLASI response to 300 mg S95021 Q2W SC in the 241 VPs matching clusters C1 to C4. The average decrease in CLASI was found to be high in C1-, C2- and C4-like VPs (Figure 6C). Surprisingly, the CLASI response to the anti-IFNα mAb response was predicted to be lower among the C3-like VPs (high interferon) (Figure 6C). This translated in > 80% of responders to S95021 in VPs matching PRECISESADS clusters 1, 2, and 4 but only ∼31% of CLASI-A responders for C3-like VPs (Figure 6D).

In agreement with results from the decision tree analysis, the C3-like VPs matching C3 patients with the highest levels of

Figure 4. Multiomics profiling of PRECISESADS lupus patients reveals four distinct clusters

(A) Workflow of clustering methodology and multiomics characterization. See STAR Methods for details.

(B) Heatmap performed on lupus patients' biological, clinical, cytokine, flow cytometry, and IFN score measurements showing the main biomarkers differentiating each molecular cluster. Each biomarker has been scaled $((x - mean(x))/(sd(x)))$ to have comparable measures. Red represents biomarker over-expression and blue biomarker under-expression. cFLC: circulating free light chains.

A

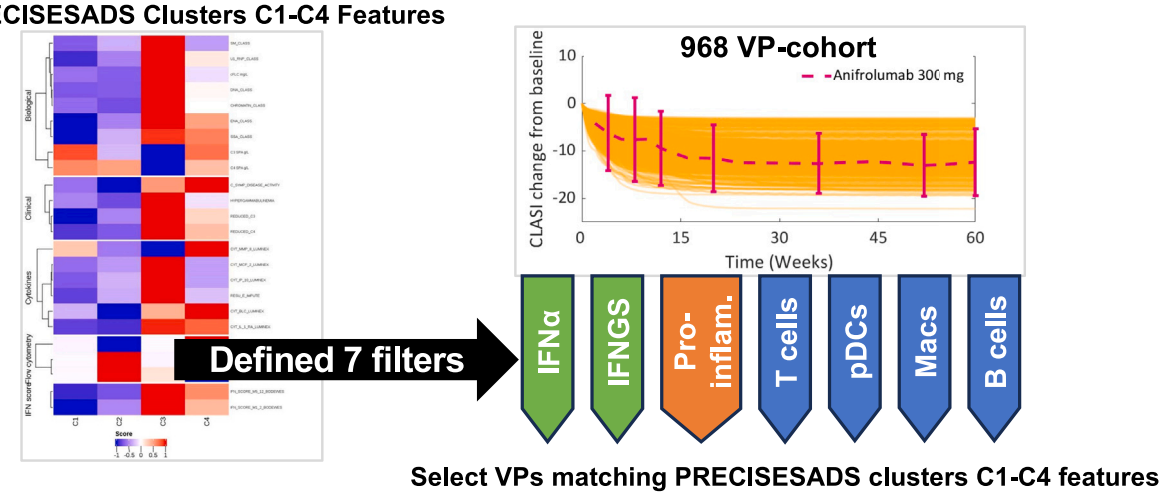

B

PRECISESADS biomarker	QSP Model Species	Cluster 1 Undefined	Cluster 2 Lymphoid	Cluster 3 Interferon	Cluster 4 Inflammatory
IFN_ALPHA	Skin IFNα	Very Low (<0.3x*)	Low (0.3-0.8x)	Hi (>3x)	Med (0.8-3x)
IFNGS_PRECISESADS	Skin Bound_IFNAR	Very Low (<0.3x)	Low (0.3-0.8x)	Hi (>3x)	Med (0.8-3x)
TNF_ALPHA	Skin pro-inflam. mediators	Low (0.5-1x)	Very Low (<0.5x)	Hi (>1.5x)	Med (1-1.5x)
CD3P_TCELLS#	Skin T cell	Med (0.5-1.5x)	Low (<0.5x)	Med (0.5-1.5x)	Hi (>1.5x)
PDC#	Skin pDCs	Med (0.8-1.5x)	Low (<0.8x)	Hi (>1.5x)	Hi (>1.5x)
CD14P_MONOCYTES#	Skin Mac	Med (0.5-1.5x)	Low (<0.5x)	Med (0.5-1.5x)	Hi (>1.5x)
CD19P_BCELLS#	Skin B cell	Med (0.5-1.5x)	Low (<0.5x)	Med (0.5-1.5x)	Hi (>1.5x)
Number of VPs identified in the 968-VPop		119	11	84	27

* 1x is defined as the species value of the average reference VP.
# absolute blood cell counts; assumed to be inversely proportional to cell numbers in the skin as measure in the model (i.e low blood cell counts corresponds to increased skin cell numbers)

Figure 5. Selection of 241 VPs in the Vpop matching the four PRECISESADS clusters

(A) Workflow for the identification of VPs matching the features characteristic of the PRECISESADS lupus patients' clusters C1–C4.

(B) PRECISESADS lupus patient features and matching QSP model species used to filter the 968 Vpop and select VPs based on the very low, low, medium, and high thresholds defined relative to the baseline value in the reference VP.

IFN/IFNAR were the least responsive to 300 mg S95021 (Figure 6C and 6D), suggesting that in this cluster, the level of IFN pathway inhibition may not be sufficient to achieve clinical response. VPs matching cluster C2 (lymphoid) and cluster C4 (inflammatory) improved the most with S95021 treatment. A strong type I IFN inhibition is thus predicted to reduce globally the inflammatory processes in these C2 and C4 phenotypes, thereby leading to anticipated significant clinical responses.

DISCUSSION

Despite recent advances, more efficient treatment strategies are needed to better manage lupus patients. In light of the known patient heterogeneity in this complex autoimmune disease, targeted therapies tailored to the specificities of well-defined patient subsets are required. To address this challenge, we used an innovative translational medicine approach that integrates multiomics profiling of large patient cohorts with quantitative systems pharmacology simulation of cutaneous lupus pathophysiology. Given the well-documented upregulation of the type I IFN pro-inflammatory pathway in a majority of lupus patients, we applied this methodology to predict the efficacy of the pan-neutralizing anti-IFNα S95021 monoclonal antibody, across patient heterogeneity.

We established a QSP model of SLE that correlates cellular and soluble proinflammatory mediators in the blood, lymph nodes, and skin with disease manifestations forming the cutaneous severity score (CLASI). To validate the model, we confirmed its ability to accurately simulate the time course of CLASI responses reported in clinical studies evaluating the anti-type I IFN receptor anifrolumab. Leveraging this mechanistic QSP model, we further forecasted the efficacy of the S95021 antibody

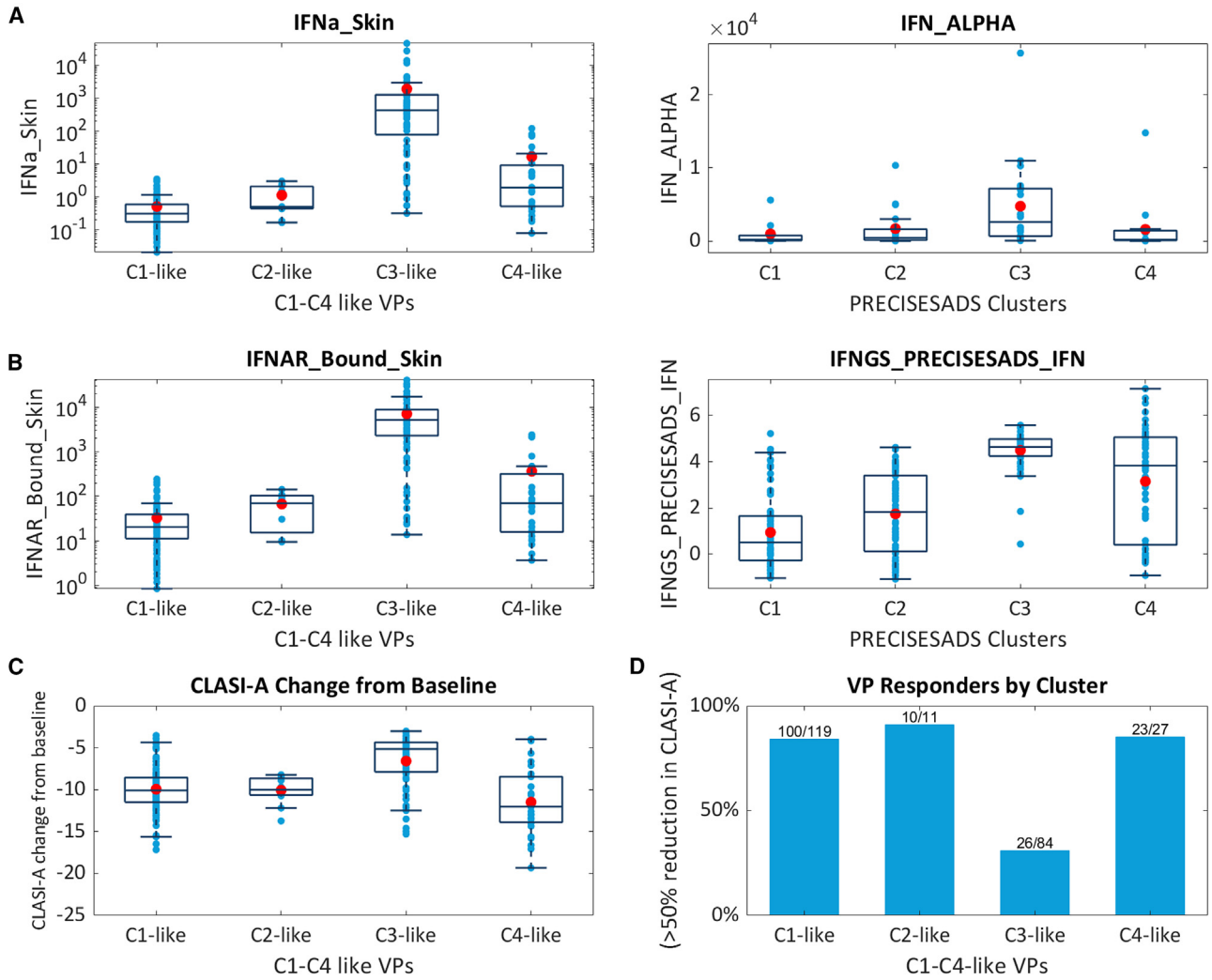

Figure 6. VPs matching clusters C1-C4 patients features have different simulated CLASI-A response to S95021

(A) Baseline skin IFNα distribution in the C1–C4-like VPs (left panel) are consistent with the relative differences in plasma IFNα measured in lupus patients from the PRECISESADS C1-C4 clusters (right panel). Boxplots with boxes representing median, Q1-Q3 interquartile range, min-max without outliers (error bars), mean (red dot) and individual VP or patient's data (blue dots).

(B) Baseline skin bound IFNAR distribution in the C1–C4-like VPs (left panel) are consistent with the relative differences in interferon gene signature (IFNGS) measured in lupus patients from the PRECISESADS C1–C4 clusters (right panel).

(C) Simulated CLASI-A response to 300 mg S95021 Q2W SC + placebo in the C1–C4-like VPs.

(D) Percentages of S95021 responders among the C1–C4-like VPs. Number of responder VPs over the total VP count per cluster are indicted. Responder VPs are defined as VPs with greater than 50% decrease in CLASI-A relative to their baseline score with 300 mg S95021 treatment.

in treating cutaneous lupus. Our predictions suggest that S95021 could match the efficacy of anifrolumab, particularly with dosing regimens of 300 mg or higher. Altogether, our study further underscores the relevance of targeting the IFN pathway in cutaneous lupus.[7–14,53]

One of the primary advantages of the QSP model is its capacity to generate thousands of virtual patients by modulating the contribution of different parameters, e.g., cell types and mediators, to clinical symptoms, thereby enabling predictions of drug efficacy at an individual patient level[54] With recent advancements in QSP modeling coupled with artificial intelligence,[39,55] the predictive data from these virtual patient cohorts can be efficiently analyzed using machine learning to differentiate between responders and non-responders. It remains crucial to thoroughly validate computational predictive models by ensuring consistency between predicted outputs and empirical data. In the present study, both the magnitude and the time course of anifrolumab responses reported in clinical studies in cutaneous lupus were closely reproduced by the model. Also, the selection of virtual patients was directly inspired from real patients, based upon data available in the literature.

To further ensure that the design of a cohort of virtual patients accurately reflects disease heterogeneity, we performed

a comprehensive molecular profiling of 337 lupus patients and 330 matched healthy controls from the PRECISESADS cohort. Integrated analysis of multiomics data identified four distinct clusters of lupus patients, highlighting the upregulation of the IFN type I pathway in a majority of these patients, while further revealing distinct patterns of immune dysregulation involving B lymphocytes and autoantibodies, as well as T cells and neutrophils, depending upon patients. Whereas transcriptomics data documenting dysregulated biological processes in the blood of PRECISESADS patients were used to identify homogeneous clusters, these transcriptomics datasets cannot be directly incorporated into QSP models. We therefore used cytokine and chemokine quantification, as well as deep immunophenotyping data from actual patients to define filters for selecting 241 virtual patients from the Vpop mirroring the heterogeneity observed across the four PRECISESADS clusters. The analysis in this VP cohort predicted differences between clusters of patients in their simulated response to S95021. Furthermore, machine learning analysis of predicted responder vs. non responder VPs in the Vpop identified candidate-biomarkers for patient selection in future clinical studies. Notably, decision tree ensemble analysis established that skin pro-inflammatory mediators (including chemokines), IFNs/IFNAR signaling, and cellular infiltrates by effector T cells in skin and lymph nodes are predictors of S95021 responses. Additionally, our study in virtual patients uncovered unexpected findings, such as the association between high levels of IFNα or bound IFNAR:IFNα complexes and low CLASI response to 300 mg S95021, suggesting the need for higher dosing regimens of the drug-candidate in patients with a strong involvement of the type I IFN pathway. The latter prediction may also provide an explanation to the limited correlation between circulating IFNα levels and responses to anifrolumab observed in clinical studies.[6]

Collectively, the integration of molecular profiling with QSP simulation of virtual patient cohorts offers a robust approach to elucidate patient heterogeneity in lupus. By predicting drug responses at an individual patient level and informing dosing regimens, this translational approach to precision medicine holds promise for optimizing treatment strategies as it applies to any complex chronic disease. Our study emphasizes the importance of leveraging multiomics profiling and predictive modeling to generate working hypotheses, obviously to be further corroborated in real-world clinical studies. In this regard, by providing candidate biomarkers as well as criteria to select patients to be included in confirmatory clinical trials, predictive modeling of drug response in virtual patients can significantly facilitate the design of future trials, while increasing their probability of success.

Limitations of the study

The QSP model described in this study is limited to cutaneous lupus, and it cannot be applied to patients with systemic lupus, for example to predict drug efficacy against kidney or lung disease. Also, the placebo effect reflected in the modeling platform represents a general immunosuppressive effect associated with steroids. This generic placebo effect does not display the same degree of variability in responses observed in actual patient populations exposed to other immunosuppressive drugs distinct from steroids, as background therapies.

RESOURCE AVAILABILITY

Lead contact

Further information and requests for resources should be directed to the lead contact, Philippe Moingeon (philippe.moingeon@universite-paris-saclay.fr).

Materials availability

This study did not generate any unique reagents/materials. Key resources used in the present study are listed in the STAR Methods, as well as in Tables S1A, S1B, S1C, S1D, S1E, and S1F and S8.

Data and code availability

Data availability

- Data used in the present study can be accessed from sources listed in the key resources table.
- Data used to define species and parameters used in QSP model were found in the literature and listed in Tables S1A, S1B, S1C, S1D, S1E, and S1F, with references provided at the end of supplemental information.
- The PRECISESADS dataset was used for clustering analysis and listed in the key resources table. The raw data are the property of the PRECISESADS consortium and are protected under the European General Data Protection Regulation (GDPR). The PRECISESADS Consortium is committed to secure patient data access through the ELIXIR platform. This commitment was given by written agreement to all patients and to the involved Ethical Committees. PRECISESADS data are hosted by ELIXIR Luxembourg and available under controlled access at: https://doi.org/10.17881/th9v-xt85. Access can be requested from the data stewardship team of ELIXIR Luxembourg via lcsb-datastewards@uni.lu. The future use of the Project database was framed according to the scope of the patient information and consent forms, where the use of patient data is open to scientific research in autoimmune diseases, for-non profit use only.

Code availability

- This study did not generate original code. We used publicly available software listed with appropriate citations in the key resources table for all the analyses listed.

Other items availability

- Any additional information required to reanalyze the data reported in this paper is available from the lead contact upon request.

ACKNOWLEDGMENTS

The study was funded by Servier. We thank the PRECISESADS consortium for providing access to multiomics data from lupus patients and healthy volunteers.

AUTHOR CONTRIBUTIONS

V.H., M.R., G.G., and P.M. were involved in study conceptualization and supervision; R.M., K.D., R.S., C.F., M.A.R., A.A., S.F. in methodology and validation; M.A.R. in providing access to study materials; P.S., K.D., G.G., M.R., L.C., L.L., S.H., and E.D. in formal analysis. P.M., V.H., and P.S. wrote the original draft and all other authors contributed to reviewing and editing the manuscript.

DECLARATION OF INTERESTS

The authors declare no competing interests. V.H., R.M., K.D., R.S., C.F., and M.R. are employees at Rosa and Co. P.S., G.G., L.L., A.A., L.C., S.F., S.H., E.D., and P.M. are—or have been—employees at Servier. Those links with for-profit companies did not influence the content of the manuscript, nor did it affect the objectives of the study.

STAR★METHODS

Detailed methods are provided in the online version of this paper and include the following:

- KEY RESOURCES TABLE
- EXPERIMENTAL MODEL AND STUDY PARTICIPANT DETAILS
  - Human subjects
- METHOD DETAILS
  - SLE QSP model development
  - Anti-IFN drugs and standard of care implementation in the platform
  - Reference VP definition and CLASI clinical score calibration
  - Virtual population creation
  - SLE patients phenotypic clustering
  - Machine learning
  - Mapping of virtual patients to PRECISESADS patient clusters
- QUANTIFICATION AND STATISTICAL ANALYSIS
  - Datasets used in this study
  - Statistical analysis

SUPPLEMENTAL INFORMATION

Supplemental information can be found online at https://doi.org/10.1016/j.isci.2025.111754.

Received: April 12, 2024
Revised: September 26, 2024
Accepted: January 3, 2025
Published: January 6, 2025

REFERENCES

1. Kaul, A., Gordon, C., Crow, M.K., Touma, Z., Urowitz, M.B., van Vollenhoven, R., Ruiz-Irastorza, G., and Hughes, G. (2016). Systemic lupus erythematosus. Nat. Rev. Dis. Primers *2*, 16039. https://doi.org/10.1038/nrdp.2016.39.
2. Fugger, L., Jensen, L.T., and Rossjohn, J. (2020). Challenges, Progress, and Prospects of Developing Therapies to Treat Autoimmune Diseases. Cell *181*, 63–80. https://doi.org/10.1016/j.cell.2020.03.007.
3. Miyagawa, I., Kubo, S., and Tanaka, Y. (2020). A wide perspective of targeted therapies for precision medicine in autoimmune diseases. Expert Rev. Precis. Med. Drug Dev. *5*, 447–453. https://doi.org/10.1080/23808993.2020.1804867.
4. Tanaka, Y. (2020). State-of-the-art treatment of systemic lupus erythematosus. Int. J. Rheum. Dis. *23*, 465–471. https://doi.org/10.1111/1756-185X.13817.
5. van Schaik, M., Arends, E.J., Soonawala, D., van Ommen, E., de Leeuw, K., Limper, M., van Paassen, P., Huizinga, T.W.J., Toes, R.E.M., van Kooten, C., et al. (2022). Efficacy of belimumab combined with rituximab in severe systemic lupus erythematosus: study protocol for the phase 3, multicenter, randomized, open-label Synbiose 2 trial. Trials *23*, 939. https://doi.org/10.1186/s13063-022-06874-w.
6. Bruce, I.N., Nami, A., Schwetje, E., Pierson, M.E., Rouse, T., Chia, Y.L., Kuruvilla, D., Abreu, G., Tummala, R., and Lindholm, C. (2021). Pharmacokinetics, pharmacodynamics, and safety of subcutaneous anifrolumab in patients with systemic lupus erythematosus, active skin disease, and high type I interferon gene signature: a multicentre, randomised, double-blind, placebo-controlled, phase 2 study. Lancet. Rheumatol. *3*, e101–e110. https://doi.org/10.1016/s2665-9913(20)30342-8.
7. Furie, R., Khamashta, M., Merrill, J.T., Werth, V.P., Kalunian, K., Brohawn, P., Illei, G.G., Drappa, J., Wang, L., and Yoo, S.; CD1013 Study Investigators (2017). Anifrolumab, an Anti-Interferon-alpha Receptor Monoclonal Antibody, in Moderate-to-Severe Systemic Lupus Erythematosus. Arthritis Rheumatol. *69*, 376–386. https://doi.org/10.1002/art.39962.
8. Furie, R.A., Morand, E.F., Bruce, I.N., Manzi, S., Kalunian, K.C., Vital, E.M., Lawrence Ford, T., Gupta, R., Hiepe, F., Santiago, M., et al. (2019). Type I interferon inhibitor anifrolumab in active systemic lupus erythematosus (TULIP-1): a randomised, controlled, phase 3 trial. Lancet. Rheumatol. *1*, e208–e219. https://doi.org/10.1016/S2665-9913(19)30076-1.
9. Morand, E.F., Furie, R., Tanaka, Y., Bruce, I.N., Askanase, A.D., Richez, C., Bae, S.C., Brohawn, P.Z., Pineda, L., Berglind, A., et al. (2020). Trial of Anifrolumab in Active Systemic Lupus Erythematosus. N. Engl. J. Med. *382*, 211–221. https://doi.org/10.1056/NEJMoa1912196.
10. Vital, E.M., Merrill, J.T., Morand, E.F., Furie, R.A., Bruce, I.N., Tanaka, Y., Manzi, S., Kalunian, K.C., Kalyani, R.N., Streicher, K., et al. (2022). Anifrolumab efficacy and safety by type I interferon gene signature and clinical subgroups in patients with SLE: post hoc analysis of pooled data from two phase III trials. Ann. Rheum. Dis. *81*, 951–961.
11. Duguet, F., Ortega-Ferreira, C., Fould, B., Darville, H., Berger, S., Chomel, A., Leclerc, G., Kisand, K., Haljasmägi, L., Hayday, A.C., et al. (2021). S95021, a novel selective and pan-neutralizing anti interferon alpha (IFN-alpha) monoclonal antibody as a candidate treatment for selected autoimmune rheumatic diseases. J. Transl. Autoimmun. *4*, 100093. https://doi.org/10.1016/j.jtauto.2021.100093.
12. De Ceuninck, F., Duguet, F., Aussy, A., Laigle, L., and Moingeon, P. (2021). IFN-alpha: A key therapeutic target for multiple autoimmune rheumatic diseases. Drug Discov. Today *26*, 2465–2473. https://doi.org/10.1016/j.drudis.2021.06.010.
13. Sim, T.M., Ong, S.J., Mak, A., and Tay, S.H. (2022). Type I Interferons in Systemic Lupus Erythematosus: A Journey from Bench to Bedside. Int. J. Mol. Sci. *23*, 2505. https://doi.org/10.3390/ijms23052505.
14. Postal, M., Vivaldo, J.F., Fernandez-Ruiz, R., Paredes, J.L., Appenzeller, S., and Niewold, T.B. (2020). Type I interferon in the pathogenesis of systemic lupus erythematosus. Curr. Opin. Immunol. *67*, 87–94. https://doi.org/10.1016/j.coi.2020.10.014.
15. Castellini-Pérez, O., Povedano, E., Barturen, G., et al.; PRECISESADS Clinical Consortium, PRECISESADS FLOW Cytometry Study Group (2024). Molecular subtypes explain lupus epigenomic heterogeneity unveiling new regulatory genetic risk variants. NPJ Genom. Med. *9*, 38. https://doi.org/10.1038/s41525-024-00420-0.
16. Guthridge, J.M., Lu, R., Tran, L.T.H., Arriens, C., Aberle, T., Kamp, S., Munroe, M.E., Dominguez, N., Gross, T., DeJager, W., et al. (2020). Adults with systemic lupus exhibit distinct molecular phenotypes in a cross-sectional study. EClinicalMedicine *20*, 100291. https://doi.org/10.1016/j.eclinm.2020.100291.
17. Haynes, W.A., Haddon, D.J., Diep, V.K., Khatri, A., Bongen, E., Yiu, G., Balboni, I., Bolen, C.R., Mao, R., Utz, P.J., and Khatri, P. (2020). Integrated, multicohort analysis reveals unified signature of systemic lupus erythematosus. JCI Insight *5*, e122312–e122320. https://doi.org/10.1172/jci.insight.122312.
18. Aringer, M., and Johnson, S.R. (2020). Classifying and diagnosing systemic lupus erythematosus in the 21st century. Rheumatology *59*, v4–v11. https://doi.org/10.1093/rheumatology/keaa379.
19. Gatto, M., Saccon, F., Zen, M., Regola, F., Fredi, M., Andreoli, L., Tincani, A., Urban, M.L., Emmi, G., Ceccarelli, F., et al. (2020). Early Disease and Low Baseline Damage as Predictors of Response to Belimumab in Patients With Systemic Lupus Erythematosus in a Real-Life Setting. Arthritis Rheumatol. *72*, 1314–1324. https://doi.org/10.1002/art.41253.
20. Allen, M.E., Rus, V., and Szeto, G.L. (2021). Leveraging Heterogeneity in Systemic Lupus Erythematosus for New Therapies. Trends Mol. Med. *27*, 152–171. https://doi.org/10.1016/j.molmed.2020.09.009.
21. Nehar-Belaid, D., Hong, S., Marches, R., Chen, G., Bolisetty, M., Baisch, J., Walters, L., Punaro, M., Rossi, R.J., Chung, C.H., et al. (2020). Mapping systemic lupus erythematosus heterogeneity at the single-cell level. Nat. Immunol. *21*, 1094–1106. https://doi.org/10.1038/s41590-020-0743-0.
22. Nguyen, Y., Nocturne, G., Henry, J., Ng, W.-F., Belkhir, R., Desmoulins, F., Bergé, E., Morel, J., Perdriger, A., Dernis, E., et al. (2024). Identification of distinct subgroups of Sjogren's disease by cluster analysis based on

clinical and biological manifestations: data from the cross-sectional Paris-Saclay and the prospective ASSESS cohorts. Lancet. Rheumatol. *6*, E216–E225. https://doi.org/10.1016/S2665-9913(23)00340-5.

23. Soret, P., Le Dantec, C., Desvaux, E., Foulquier, N., Chassagnol, B., Hubert, S., Jamin, C., Barturen, G., Desachy, G., Devauchelle-Pensec, V., et al. (2021). A new molecular classification to drive precision treatment strategies in primary Sjogren's syndrome. Nat. Commun. *12*, 3523. https://doi.org/10.1038/s41467-021-23472-7.
24. Moingeon, P. (2023). Artificial intelligence-driven drug development against autoimmune diseases. Trends Pharmacol. *44*, 411–424.
25. Desvaux, E., Aussy, A., Hubert, S., Keime-Guibert, F., Blesius, A., Soret, P., Guedj, M., Pers, J.O., Laigle, L., and Moingeon, P. (2022). Model-based computational precision medicine to develop combination therapies for autoimmune diseases. Expert Rev. Clin. Immunol. *18*, 47–56. https://doi.org/10.1080/1744666X.2022.2012452.
26. Toro-Dominguez, D., and Alarcon-Riquelme, M.E. (2021). Precision medicine in autoimmune diseases: fact or fiction. Rheumatology *60*, 3977–3985. https://doi.org/10.1093/rheumatology/keab448.
27. Fasano, S., Milone, A., Nicoletti, G.F., Isenberg, D.A., and Ciccia, F. (2023). Precision medicine in systemic lupus erythematosus. Nat. Rev. Rheumatol. *19*, 331–342. https://doi.org/10.1038/s41584-023-00948-y.
28. Guthridge, J.M., Wagner, C.A., and James, J.A. (2022). The promise of precision medicine in rheumatology. Nat. Med. *28*, 1363–1371. https://doi.org/10.1038/s41591-022-01880-6.
29. Banchereau, R., Hong, S., Cantarel, B., Baldwin, N., Baisch, J., Edens, M., Cepika, A.M., Acs, P., Turner, J., Anguiano, E., et al. (2016). Personalized Immunomonitoring Uncovers Molecular Networks that Stratify Lupus Patients. Cell *165*, 551–565. https://doi.org/10.1016/j.cell.2016.03.008.
30. Barturen, G., Beretta, L., Cervera, R., Van Vollenhoven, R., and Alarcón-Riquelme, M.E. (2018). Moving towards a molecular taxonomy of autoimmune rheumatic diseases. Nat. Rev. Rheumatol. *14*, 75–93. https://doi.org/10.1038/nrrheum.2017.220.
31. Barturen, G., Babaei, S., Català-Moll, F., Martínez-Bueno, M., Makowska, Z., Martorell-Marugán, J., Carmona-Sáez, P., Toro-Domínguez, D., Carnero-Montoro, E., Teruel, M., et al. (2021). Integrative Analysis Reveals a Molecular Stratification of Systemic Autoimmune Diseases. Arthritis Rheumatol. *73*, 1073–1085. https://doi.org/10.1002/art.41610.
32. Huang, X., Luu, L.D.W., Jia, N., Zhu, J., Fu, J., Xiao, F., Liu, C., Li, S., Shu, G., Hou, J., et al. (2022). Multi-Platform Omics Analysis Reveals Molecular Signatures for Pathogenesis and Activity of Systemic Lupus Erythematosus. Front. Immunol. *13*, 833699. https://doi.org/10.3389/fimmu.2022.833699.
33. Chu, X., Zhang, B., Koeken, V.A.C.M., Gupta, M.K., and Li, Y. (2021). Multi-Omics Approaches in Immunological Research. Front. Immunol. *12*, 668045. https://doi.org/10.3389/fimmu.2021.668045.
34. Anchang, C.G., Xu, C., Raimondo, M.G., Atreya, R., Maier, A., Schett, G., Zaburdaev, V., Rauber, S., and Ramming, A. (2021). The Potential of OMICs Technologies for the Treatment of Immune-Mediated Inflammatory Diseases. Int. J. Mol. Sci. *22*, 7506. https://doi.org/10.3390/ijms22147506.
35. Moingeon, P., Kuenemann, M., and Guedj, M. (2022). Artificial intelligence-enhanced drug design and development: Toward a computational precision medicine. Drug Discov. Today *27*, 215–222. https://doi.org/10.1016/j.drudis.2021.09.006.
36. Friedrich, C.M. (2016). A model qualification method for mechanistic physiological QSP models to support model-informed drug development. CPT Pharmacometrics Syst. Pharmacol. *5*, 43–53. https://doi.org/10.1002/psp4.12056.
37. Bradshaw, E.L., Spilker, M.E., Zang, R., Bansal, L., He, H., Jones, R.D.O., Le, K., Penney, M., Schuck, E., Topp, B., et al. (2019). Applications of Quantitative Systems Pharmacology in Model-Informed Drug Discovery: Perspective on Impact and Opportunities. CPT Pharmacometrics Syst. Pharmacol. *8*, 777–791. https://doi.org/10.1002/psp4.12463.
38. Nijsen, M.J.M.A., Wu, F., Bansal, L., Bradshaw-Pierce, E., Chan, J.R., Liederer, B.M., Mettetal, J.T., Schroeder, P., Schuck, E., Tsai, A., et al. (2018). Preclinical QSP Modeling in the Pharmaceutical Industry: An IQ Consortium Survey Examining the Current Landscape. CPT Pharmacometrics Syst. Pharmacol. *7*, 135–146. https://doi.org/10.1002/psp4.12282.
39. Aghamiri, S.S., Amin, R., and Helikar, T. (2022). Recent applications of quantitative systems pharmacology and machine learning models across diseases. J. Pharmacokinet. Pharmacodyn. *49*, 19–37. https://doi.org/10.1007/s10928-021-09790-9.
40. Myers, R.C., Augustin, F., Huard, J., and Friedrich, C.M. (2023). Using machine learning surrogate modeling for faster QSP VP cohort generation. CPT Pharmacometrics Syst. Pharmacol. *12*, 1047–1059. https://doi.org/10.1002/psp4.12999.
41. Ramakrishnan, V., Friedrich, C., Witt, C., Sheehan, R., Pryor, M., Atwal, J.K., Wildsmith, K., Kudrycki, K., Lee, S.H., Mazer, N., et al. (2023). Quantitative systems pharmacology model of the amyloid pathway in Alzheimer's disease: Insights into the therapeutic mechanisms of clinical candidates. CPT Pharmacometrics Syst. Pharmacol. *12*, 62–73. https://doi.org/10.1002/psp4.12876.
42. Rullmann, J.A.C., Struemper, H., Defranoux, N.A., Ramanujan, S., Meeuwisse, C.M.L., and van Elsas, A. (2005). Systems biology for battling rheumatoid arthritis: application of the Entelos PhysioLab platform. Syst. Biol. *152*, 256–262. https://doi.org/10.1049/ip-syb:20050053.
43. Meeuwisse, C.M., van der Linden, M.P., Rullmann, T.A., Allaart, C.F., Nelissen, R., Huizinga, T.W., Garritsen, A., Toes, R.E., van Schaik, R., and van der Helm-van Mil, A.H. (2011). Identification of CXCL13 as a marker for rheumatoid arthritis outcome using an in silico model of the rheumatic joint. Arthritis Rheum. *63*, 1265–1273. https://doi.org/10.1002/art.30273.
44. Balbas-Martinez, V., Asin-Prieto, E., Parra-Guillen, Z.P., and Troconiz, I.F. (2020). A Quantitative Systems Pharmacology Model for the Key Interleukins Involved in Crohn's Disease. J. Pharmacol. Exp. Ther. *372*, 299–307. https://doi.org/10.1124/jpet.119.260539.
45. Rogers, K.V., Martin, S.W., Bhattacharya, I., Singh, R.S.P., and Nayak, S. (2021). A Dynamic Quantitative Systems Pharmacology Model of Inflammatory Bowel Disease: Part 2 - Application to Current Therapies in Crohn's Disease. Clin. Transl. Sci. *14*, 249–259. https://doi.org/10.1111/cts.12850.
46. Miyano, T., Irvine, A.D., and Tanaka, R.J. (2022). A mathematical model to identify optimal combinations of drug targets for dupilumab poor responders in atopic dermatitis. Allergy *77*, 582–594. https://doi.org/10.1111/all.14870.
47. Go, N., Arsene, S., Faddeenkov, I., Galland, T., Martis, B.S., Lefaudeux, D., Wang, Y., Etheve, L., Jacob, E., Monteiro, C., et al. (2024). A quantitative systems pharmacology workflow towards optimal design and biomarker stratification of atopic dermatitis clinical trials. J. Allergy Clin. Immunol. *153*, 1330–1343. https://doi.org/10.1016/j.jaci.2023.12.031.
48. Bruce, I., Nami, A., Schwetje, E., Pierson, M., Chia, Y., Kuruvilla, D., Abreu, G., Tummala, R., and Lindholm, C. (2019). PK/PD, Safety and Exploratory Efficacy of Subcutaneous Anifrolumab in SLE: A Phase-II Study in Interferon Type I High Patients with Active Skin Disease. Arthritis Rheumatol. *71*, 2563.
49. AlE'ed, A., Aydin, P.O.A., Al Mutairi, N., AlSaleem, A., Sonmez, H.E., Henrickson, M., Huggins, J.L., Ozen, S., Al-Mayouf, S.M., and Brunner, H.I. (2018). Validation of the Cutaneous Lupus Erythematosus Disease Area and Severity Index and pSkindex27 for use in childhood-onset systemic lupus erythematosus. Lupus Sci. Med. *5*, e000275. https://doi.org/10.1136/lupus-2018-000275.
50. Mucke, J., Alarcon-Riquelme, M., Andersen, J., Aringer, M., Bombardieri, S., Brinks, R., Cervera, R., Chehab, G., Cornet, A., Costedoat-Chalumeau, N., et al. (2021). What are the topics you care about making trials in lupus more effective? Results of an Open Space meeting of international lupus experts. Lupus Sci. Med. *8*, e000506. https://doi.org/10.1136/lupus-2021-000506.
51. Figueroa-Parra, G., Putman, M.S., Crowson, C.S., and Duarte-García, A. (2024). Fragility of randomised controlled trials for systemic lupus

erythematosus and lupus nephritis therapies. Lupus Sci. Med. *11*, e001068. https://doi.org/10.1136/lupus-2023-001068.

52. Chiche, L., Jourde-Chiche, N., Whalen, E., Presnell, S., Gersuk, V., Dang, K., Anguiano, E., Quinn, C., Burtey, S., Berland, Y., et al. (2014). Modular transcriptional repertoire analyses of adults with systemic lupus erythematosus reveal distinct type I and type II interferon signatures. Arthritis Rheumatol. *66*, 1583–1595. https://doi.org/10.1002/art.38628.
53. Bruera, S., Chavula, T., Madan, R., and Agarwal, S.K. (2022). Targeting type I interferons in systemic lupus erythematous. Front. Pharmacol. *13*, 1046687. https://doi.org/10.3389/fphar.2022.1046687.
54. Moingeon, P., Chenel, M., Rousseau, C., Voisin, E., and Guedj, M. (2023). Virtual patients, digital twins and causal disease models: Paving the ground for in silico clinical trials. Drug Discov. Today *28*, 103605. https://doi.org/10.1016/j.drudis.2023.103605.
55. Zhang, T., Androulakis, I.P., Bonate, P., Cheng, L., Helikar, T., Parikh, J., Rackauckas, C., Subramanian, K., and Cho, C.R.; Working Group (2022). Two heads are better than one: current landscape of integrating QSP and machine learning : An ISoP QSP SIG white paper by the working group on the integration of quantitative systems pharmacology and machine learning. J. Pharmacokinet. Pharmacodyn. *49*, 5–18. https://doi.org/10.1007/s10928-022-09805-z.
56. Wang, B., Higgs, B.W., Chang, L., Vainshtein, I., Liu, Z., Streicher, K., Liang, M., White, W.I., Yoo, S., Richman, L., et al. (2013). Pharmacogenomics and translational simulations to bridge indications for an anti-interferon-alpha receptor antibody. Clin. Pharmacol. Ther. *93*, 483–492. https://doi.org/10.1038/clpt.2013.35.
57. Tummala, R., Rouse, T., Berglind, A., and Santiago, L. (2018). Safety, tolerability and pharmacokinetics of subcutaneous and intravenous anifrolumab in healthy volunteers. Lupus Sci. Med. *5*, e000252. https://doi.org/10.1136/lupus-2017-000252.
58. Shah, D.K., and Betts, A.M. (2013). Antibody biodistribution coefficients: inferring tissue concentrations of monoclonal antibodies based on the plasma concentrations in several preclinical species and human. mAbs *5*, 297–305. https://doi.org/10.4161/mabs.23684.
59. Albrecht, J., Taylor, L., Berlin, J.A., Dulay, S., Ang, G., Fakharzadeh, S., Kantor, J., Kim, E., Militello, G., McGinnis, K., et al. (2005). The CLASI (Cutaneous Lupus Erythematosus Disease Area and Severity Index): an outcome instrument for cutaneous lupus erythematosus. J. Invest. Dermatol. *125*, 889–894. https://doi.org/10.1111/j.0022-202X.2005.23889.x.
60. Ortega-Ferreira, C., Soret, P., Robin, G., Speca, S., Hubert, S., Le Gall, M., Desvaux, E., Jendoubi, M., Saint-Paul, J., Chadli, L., et al. (2023). Antibody-mediated neutralization of galectin-3 as a strategy for the treatment of systemic sclerosis. Nat. Commun. *14*, 5291. https://doi.org/10.1038/s41467-023-41117-9.

STAR★METHODS

KEY RESOURCES TABLE

REAGENT or RESOURCE	SOURCE	IDENTIFIER
Deposited data		
Patients' data (demographics)	This paper	Table S8
Patients' data (measurements)	This paper	Table S8
SLE Platform Species	This paper	Tables S1A
SLE Platform Parameters	This paper	Table S1B
SLE Platform Equations	This paper	Tables S1E and S1F
PRECISESADS data	PRECISESADS consortium	https://doi.org/10.17881/th9v-xt85
Software and algorithms		
MATLAB R2020a	MathWorks (Natick, MA)	https://www.mathworks.com/products/matlab.html
SimBiology	MathWorks (Natick, MA)	https://www.mathworks.com/products/simbiology.html
Statistics and Machine Learning toolbox	MathWorks (Natick, MA)	https://www.mathworks.com/products/statistics.html
Clustering software	R system software	http://www.R-project.org, V4.0.1

EXPERIMENTAL MODEL AND STUDY PARTICIPANT DETAILS

Human subjects

A clustering analysis was conducted on data generated from samples of lupus patients included in the European multi-center cross-sectional study of the PRECISESADS IMI consortium.[30,31] A total of 337 lupus patients and 330 healthy volonteers were included in the study. The detailed demographic and clinical information are provided in Table S8. All human subjects signed an informed consent prior to study inclusion. Recruitment was performed between December 2014 and October 2017 involving 19 institutions in 9 countries (Austria, Belgium, France, Germany, Hungary, Italy, Portugal, Spain and Switzerland). The study adhered to the standards set by International Conference on Harmonization and Good Clinical Practice (ICHGCP), and to the ethical principles derived from the Declaration of Helsinki (2013).

The Ethical Review Boards of the 19 participating institutions approved the protocol of the cross-sectional study. Ethical committees involved were: Comitato Etico Milano, Italy; Comité de Protection des Personnes Ouest VI Brest, France; Louvain, Comité d'Ethique Hospitalo-Facultaire, Belgium; Comissao de ética para a Saude—CES do CHP Porto, Portugal; Comité Ética de Investigación Clínica del Hospital Clínic de Barcelona, Spain; Commissie Medische Ethiek UZ KU Leuven/Onderzoek, Belgium; Geschaftsstelle Ethikkommission, Cologne, Germany; Ethikkommission Hannover, Germany; Ethik Kommission. Borschkegasse, Vienna, Austria; Comité de Ética e la Investigación de Centro de Granada, Spain; Commission Cantonale d'éthique de la recherche Hopitaux universitaires de Genève, Switzerland; Csongrad Megyei Kormanyhivatal, Szeged, Hungary; Ethikkommission, Berlin, Germany; Andalusian Public Health System Biobank, Granada, Spain. The cross-sectional PRECISEADS study is registered in ClinicalTrials.com with number NCT02890121. More specific details on sample and data collection are provided in the main PRECISESADS publication.[31]

METHOD DETAILS

SLE QSP model development

A mechanistic Quantitative Systems Pharmacology (QSP) SLE model was built using MathWorks MATLAB/SimBiology Software. The SLE PhysioPD Platform is a set of ordinary differential equations (ODEs; as listed in KEY RESSOURCES) representing SLE-related inflammatory processes in lymph nodes and the resulting skin damage. The model includes three mechanistic compartments: a "Blood" compartment representing the systemic circulation, a "Lymph Node" (LN) compartment and a "Skin" compartment (Figure 1A). The Blood compartment serves as a source for inactive immune cells. The LN compartment is a site of activation for immune cells, subsequently recruited to the inflamed skin. The Skin compartment is the site of the SLE-induced inflammation leading to cutaneous lesions and where the cutaneous clinical score is calculated. Based on a comprehensive literature survey, the following pathological processes relevant for the development of cutaneous lesions were included in the model, with a focus on cells and pathways regulated by type I interferons (IFNs).

(1) Keratinocyte/corneocyte cell proliferation, activation, apoptosis, differentiation and shedding,
(2) Plasmacytoid dendritic cell (pDC) recruitment into LN or skin, activation, and apoptosis,

(3) T and B cell recruitment into LN or skin, activation and differentiation into effector cells,
(4) Mediator production in LN and skin: type I IFNs, pro- and anti-inflammatory cytokines, and chemokines; autoantibodies,
(5) Regulation of cellular processes by other cell types, cytokines and IFNAR signaling,
(6) S95021 and anifrolumab pharmacokinetics, binding to IFNs, clearance from the tissues and pharmacodynamics effect in LN and skin,
(7) Steroid effects.

Model qualification, calibration, and testing against published datasets were conducted as previously described.[36] Parameters for individual processes, such as keratinocyte and immune cell numbers, and turnover rates in skin and lymph nodes were identified in the literature or calibrated based on published data (Tables S1A, S1B, S1C, S1D, and S2–S5).

Anti-IFN drugs and standard of care implementation in the platform

Drug pharmacokinetics (PK) and pharmacodynamic (PD) effects were implemented in the QSP model using parameter estimates for the anti-IFNα mAb S95021 and the anti-IFNα receptor (IFNAR) monoclonal antibody anifrolumab (Tables S1A and S1B). Anifrolumab PK was implemented as a 2-compartment model[56] with dosing in a central compartment, transport between the central and the peripheral compartment, and elimination from the central compartment. Anifrolumab PK parameters were adjusted so that simulations in the reference VP matched the anifrolumab plasma concentrations from two clinical studies.[6,57] S95021 PK was implemented as a 2-compartment model based on Servier's proprietary data (personal communication). S95021 human PK parameters were derived from Servier's PK model (Tables S1A and S1B). S95021 binding constants to IFNα were estimated from *in vitro* studies.[11] As there was no published data for the biodistribution of anifrolumab or S95021 in tissues, standard partition coefficients for therapeutic mAbs were used as a first approximation: 15.7% for the skin and 8.4% for the lymph node compartments, respectively.[58]

Placebo effect representation: A majority of patients received oral corticosteroids in anifrolumab clinical trials as background therapy in the placebo groups.[6] Continuous steady-state steroid effects were thus implemented to account for the standard of care background treatments used in the placebo groups of the anifrolumab clinical trial used to calibrate the clinical response. The effects of steroids on the various cell types were estimated from published *in vitro* studies (Table S6) and the steady-state steroid exposure (drug concentration in lymph node and skin compartments) was calibrated to achieve appropriate clinical response measured in the placebo group of anifrolumab clinical trials.[6]

Reference VP definition and CLASI clinical score calibration

The reference VP represents an average SLE patient with stable chronic cutaneous symptoms and lymph node inflammation: all cell numbers and mediator concentrations at a dynamic equilibrium are consistent with literature data for an average moderate SLE patient (Tables S1A). Clinical responses to standard dosing of anifrolumab and Placebo in the reference VP were calibrated to match the average CLASI-A response to 300 mg anifrolumab SC Q2W or placebo reported in a recent Phase 2 clinical trial[6] (Figure 1B).

The CLASI score is calculated in the QSP model as the sum of CLASI-A and CLASI-D weighted subscores per CLASI definition.[59] The CLASI subscores are calculated using linear correlation between defined model species for each individual CLASI subscore as follows.

Erythema

Erythema is a function of the state of activation of the skin vasculature and the pro-inflammatory mediators.

(1) ''Activated_Vasc'' is a dynamic species node that quantifies both the level and the quality of the vasculature and is regulated by pro-inflammatory mediators
(2) Pro-inflammatory mediators can also independently increase vascular permeability and skin ''redness''

The baseline erythema score value for the reference VP was set at 8 on a scale from 0 to 39.

Scaling

Lesioned skin scaling is a function of the number of corneocytes (CC), and abnormal desquamation measured in the QSP model by the KC_Activity calculated parameter. The baseline scaling score value for the reference VP was set at 5 on a scale from 0 to 26.

Mucus membrane lesions

Ulcerations or lesions of the mouth mucosa are common symptom in SLE and are reported as present (1) or absent (0) in the CLASI scoring sheet. As the QSP model does not include mouth mucosa-specific inflammation, this subscore is correlated with the overall CLASI subscore, as the average mucus membrane lesions score appears to be linearly proportional to the total CLASI score in patients with different disease severities. The baseline mucus membrane lesions score for the reference VP was set at 0.5 on a scale from 0 to 1.

Recent hair loss

This subscore assesses whether the patient experienced a recent (less than 30 days) hair loss (1) or not (0). This subscore is correlated with the overall CLASI score as the average recent hair loss score is linearly proportional to the total CLASI score in patients with different disease severities. The baseline recent hair loss score for the reference VP was set at 0.5 on a scale from 0 to 1.

Alopecia

The CLASI alopecia score quantifies reversible non-scarring loss of hair in SLE patients. Alopecia is calculated in the QSP model as a function of a dynamic hair follicle damage species. The baseline alopecia score for the reference VP was set at 1.5 on a scale from 0 to 3.

Dyspigmentation

Total skin pigmentation is integrated from the pigmentation levels of the various KC subtypes.

(1) The levels of pigments in each KC subtypes (i.e., Pigment_KC_Basal) is combined to calculate a relative total pigmentation of the SLE lesion,
(2) The Total_Pigmentation is used to calculate the Dyspigmentation subscore.

The baseline dyspigmentation score for the reference VP was set at 6 on a scale from 0 to 13.

Scarring

Scarring is included as a constant species to track the amount of irreversible scarring in individual patients.

(1) Scarring score is assumed to be constant for an individual patient and would not change throughout the clinical trial duration with or without treatment.

The baseline scarring score for the reference VP was set at 3 on a scale from 0 to 30.

The equations for the calculation of each individual CLASI subscores are listed in Tables S1E. The parameters use to define the slope and intercept for the linear correlation were calibrated to match the reduction in CLASI subscores from various clinical trials.[6–10]

Virtual population creation

A virtual population (VPop) was created to capture the variability in the contribution of different cell types and mediators to skin damage and inflammation. Critical parameters to vary in the model were identified, and ranges of values (lower and upper bounds) around the average parameter values defining the reference VP were estimated from published pre-clinical and clinical studies (Tables S1C). Virtual patients were generated by randomly sampling critical parameters from a uniform distribution between defined ranges, simulating parameter sets in the model for 60 weeks, and filtering virtual patients based on criteria from literature defining SLE patient characteristics (Table S1D). Virtual patients that failed to meet the defined criteria (biological constraints such as cell numbers in LN and skin, as well as range of baseline CLASI score) were eliminated. Virtual patients that met the filtering criteria, or "plausible" VPs, were then simulated with anifrolumab and steroid "placebo" therapy for 60 weeks. Sampling continued until the VPop distribution matched the mean baseline CLASI measurements as well as CLASI responses in the anifrolumab and placebo-treated patients from the Phase 2 anifrolumab trial.[6] Based on prior experience, around 1000 VPs were expected to be sufficient. After creating about 950 VPs, further additions did not significantly enhance the fit, so simulations were stopped after 968 VPs to save computational costs.

Simulations were performed in MATLAB 2020a using the SimBiology Toolbox (Mathworks, Natick, MA). The VPop follows a normal distribution around the mean for baseline CLASI score, change in CLASI score with 300 mg anifrolumab and change in CLASI score with steroid treatment. The mean and standard deviation for those 3 criteria matched the clinical trial outcomes as shown in Table S7.

SLE patients phenotypic clustering

Patient subgroup discovery was based on the pre-processed RNAseq data and clustering methodologies previously used for molecular classification of patients from the PRECISESADS cohort with either primary Sjögren syndrome[23] or systemic sclerosis.[60] Except when indicated, data analyses were carried out using either an assortment of R system software (http://www.R-project.org, V4.0.1) packages, including those of Bioconductor v3.17, or original R code. R packages are indicated when appropriate. In order to analyze RNAseq data, first, bcl2fastq2 Conversion Software v2.20 was used to demultiplex sequencing data and convert BCL files. Quality control was obtained with FastQC tools v0.11.18 and adapters were removed with Cutadapt v1.18. Transcriptome alignment was done with STAR v2.5.2b on GENCODE v19 annotation (hg19) and read counts were obtained with RSEM v1.2.31. For normalizations and batch correction, read counts were normalized by the variance stabilizing transformation vst function from the DESeq2 v1.30.0R package. To reduce the effect of the RIN, a correction was applied using the ComBat function from the sva v3.38.0R package, after categorization of RIN values into 7 classes: [6.5–7.0], [7.0–7.5], [7.5–8.0], [8.0–8.5], [8.5–9.0], [9.0–9.5], [9.5–10].

With the objective to establish a robust classification of lupus patients into homogeneous.subgroups, we used a "semi-supervised" approach combining iterates of unsupervised and supervised steps. The training set comprised 269 lupus samples and the test set comprised 68 samples.

Step 1: Unsupervised gene selection

The coefficient of variation ($CV_g = \frac{\sigma_g}{\mu_g}$, with σ_g is the standard deviation of the gene g and μ_g the mean of the gene g estimated on discovery population) and its robust version ($r\,CV_g = \frac{\gamma_g}{\mu_g}$, with γ_g is the median absolute deviation) were calculated for each gene.

Both were highly concordant. The top 25% main variants were selected to perform the subsequent clustering analysis.

Step 2: Robust consensus clustering

To determine the number of clusters, a consensus clustering between three methods was performed: (i) Agglomerative Hierarchical Clustering (hclust function from stats v4.0.2 R package) with Pearson correlation as a similarity measure and the Ward's linkage method, (ii) K-means clustering (kmeans function from stats R package) with 4 groups and (iii) Gaussian mixture clustering (mclust function from mclust v5.4.6 R package).

Step 3: Identification of molecular signature

A supervised analysis was performed on patients with consistent cluster assignments between the three clustering methods (considered as ''core'' molecular profiles), in order to identify the most discriminating signatures of the four clusters. A first signature of set of 2.291 genes was selected from a classical one-way ANOVA (FDR < 1e-10), and then reduced by Random Forest to 355 top discriminating genes (randomForest function from randomForest v4.6-14 R package).

Step 4: Robustness classification

To validate the robustness of our clustering, we re-applied the Step 2 on our discovery set and on final signatures.

Step 5: Prediction on validation test

Unconsistent patients and validation patient test were assigned to either one of the 4 clusters by applying a distance-to-centroid method based on Pearson correlation.

Machine learning

Decision tree and ensemble learning methods were used to identify model parameters and species that could discriminate between good and poor responders to therapies tested in the SLE platform. VPs achieving 50% or greater decrease in CLASI score from baseline are considered high responders using the response criteria defined in the anifrolumab Phase 2 trial.[6] VPs were classified as low or high responders based on CLASI response to 300 mg S95021 Q2W therapy at 60 weeks. Individual decision tree models were created for this classification criteria using the baseline model species values for each VP as model inputs, and responder class labels as the model response. To perform the ensemble analysis, an adaptive boosting algorithm with 56 trees was trained for the dataset, and a predictor importance algorithm was used to identify parameters in the ensemble with the most significant contributions to CLASI response. Machine learning analyses were performed using the MATLAB 2020a Statistics and Machine Learning Toolbox (Mathworks, Natick, MA).

Mapping of virtual patients to PRECISESADS patient clusters

Seven biomarkers distinguishing the PRECISADS clusters (Figure 3B) were assigned to QSP model species (Figure 5B) using reasonable scientific assumptions, as the mechanistic QSP model does not contain the exact biomarkers included in the PRECISESADS dataset. These seven biomarkers were used as filters using threshold values defined from average levels of each individual biomarker in the PRECISESADS clusters C1-C4 (Figures S2–S4). The filtering criteria was more or less stringent for each biomarker based on the ranking in the tree ensemble analysis (Figure 3).

(1) IFNα and IFNGS were the two mandatory filters, and the VPs selected matched the distribution observed in real patients from clusters C1-C4 (Figures 6A and 6B),
(2) To be selected, the VP then had to match 2 out of the 5 remaining filters (pro-inflammatory cytokines, T cells, pDCs, macrophages, B cells) which were considered less stringent, based on the lower ranking in the ensemble analysis and their less discriminative distribution in the C1-C4 clusters (Figures S5–S7).

QUANTIFICATION AND STATISTICAL ANALYSIS

Datasets used in this study

Data used to define species and parameters used in the QSP model were found in the literature and listed in Tables S1A, S1B, S1C, S1D, and S2–S6.

The PRECISESADS dataset was used for clustering analysis and listed in the key resources table.

Statistical analysis

Statistical analysis was performed in MATLAB. Anifrolumab and S95021 CLASI-A clinical response in the Vpop were compared using a T-test.

In the analysis of PRECISESADS lupus patients' descriptive statistics, statistical significance was determined by global Kruskal-Wallis test for numerical variables and by global Fisher exact test for categorical variables.